

RESEARCH ARTICLE

Open Access



# Anterior cruciate ligament reconstruction in a rabbit model using a silk-collagen scaffold modified by hydroxyapatite at both ends: a histological and biomechanical study

Fanggang Bi<sup>1\*</sup>, Yangdi Chen<sup>2</sup>, Junqi Liu<sup>3</sup>, Yafei Wang<sup>1</sup>, Danfeng Xu<sup>4</sup> and Ke Tian<sup>1</sup>

## Abstract

**Background:** To investigate osteointegration at the graft-bone interface and the prevention of osteoarthritis after anterior cruciate ligament (ACL) reconstruction using a silk-collagen scaffold with both ends modified by hydroxyapatite (HA) in a rabbit model.

**Methods:** The HA/silk-collagen scaffold was fabricated using a degummed, knitted silk scaffold, collagen I matrix, and simulated body fluid (SBF). The HA/silk-collagen scaffold was rolled up to make a graft for replacing the native ACL in the experimental group (HA group), and the silk-collagen scaffold was used in the control (S group). All specimens were harvested at 16 weeks postoperatively to evaluate graft-bone healing and osteoarthritis prevention.

**Results:** Histological staining revealed the massive formation of more mature bone at the tendon-bone interface, and immunohistochemistry staining revealed more collagen I and osteocalcin deposition in the HA group than in the S group. Higher signals indicating more bone mineral formation were detected in the HA group than in the S group, which was consistent with the results of biomechanical testing. Better osteoarthritis prevention was also observed in the HA group, indicating a more stable knee joint in the HA group than in the S group.

**Conclusion:** The HA/silk-collagen scaffold promotes osteointegration at the tendon-bone interface after ACL reconstruction and has great potential for clinical applications.

**Keywords:** Hydroxyapatite, Anterior cruciate ligament reconstruction, Tendon-bone healing, Osteointegration

## Introduction

The anterior cruciate ligament (ACL) is an important factor in maintaining stability and enabling functional movements of the knee joint. Tear or rupture of the ACL is one of the most common injuries due to its biomechanical function during sports activities. There are 100,000-200,

000 cases of ACL injury annually in the USA [1]. Since the ACL has a low capacity for regeneration, the current gold standard for treating ACL rupture is reconstruction with autografts [2]. Autografts, including hamstring grafts and bone-patellar tendon-bone grafts, have drawbacks, such as donor site morbidity, ligament laxity, and a high incidence of bone tunnel widening [3]. Alternatively, ACL reconstruction with allografts can avoid donor site morbidity for patients, but additional risks, including the risk of disease transmission, an immunogenic response, and a

\* Correspondence: [163bfg@163.com](mailto:163bfg@163.com)

<sup>1</sup>Department of Orthopedic Surgery, The First Affiliated Hospital of Zhengzhou University, NO.1 Jianshe East Road, Zhengzhou 450001, China  
Full list of author information is available at the end of the article



© The Author(s). 2021 **Open Access** This article is licensed under a Creative Commons Attribution 4.0 International License, which permits use, sharing, adaptation, distribution and reproduction in any medium or format, as long as you give appropriate credit to the original author(s) and the source, provide a link to the Creative Commons licence, and indicate if changes were made. The images or other third party material in this article are included in the article's Creative Commons licence, unless indicated otherwise in a credit line to the material. If material is not included in the article's Creative Commons licence and your intended use is not permitted by statutory regulation or exceeds the permitted use, you will need to obtain permission directly from the copyright holder. To view a copy of this licence, visit <http://creativecommons.org/licenses/by/4.0/>. The Creative Commons Public Domain Dedication waiver (<http://creativecommons.org/publicdomain/zero/1.0/>) applies to the data made available in this article, unless otherwise stated in a credit line to the data.

higher failure rate, should be considered [4]. Artificial synthetic grafts overcome some deficiencies of autografts and allografts and exhibit satisfactory results in the short term, but their long-term complications include graft rupture, chronic synovitis, foreign-body reactions, and poor tissue integration [5]. Therefore, research on ligament tissue engineering to develop an ideal biological scaffold for ACL reconstruction has become a focus in sports medicine.

An ideal biological scaffold for ACL reconstruction should be biocompatible and biodegradable, not only providing immediate joint stability but also promoting ligamentous tissue formation in the knee cavity and tendon-bone healing in the bone tunnel [2, 6]. Recently, silk-based scaffolds have been increasingly utilized for ligament regeneration because of their good biocompatibility, slow degradability, and remarkable mechanical strength [7]. The biocompatibility of silk can be promoted by degumming [8]. The combination of silk and a collagen sponge to mimic the native structure and composition of ligament extracellular matrix (ECM) exhibited satisfactory cellular infiltration and tissue regeneration. In a previous study, we fabricated a knitted silk-collagen scaffold and achieved promising results in a rabbit model of ACL reconstruction [2]. The knitted silk fibroin scaffold combined with the collagen matrix showed better neoligament regeneration and tendon-bone healing than autografts. However, the tendon-bone interface needs to be improved. Although the ingrowth of trabecular bone into the graft was observed at 16 weeks postoperatively [2], more tendon-bone healing is still required for osteointegration at the tendon-bone interface after ACL reconstruction.

Hydroxyapatite (HA) is generally known for its biocompatibility and has been proven to enhance tendon-bone healing in animal studies [9]. Methods for the surface modification of implants by HA include biomineralization, laser pulse deposition, plasma spraying, electrochemical deposition, electrophoretic deposition, and dip coating, among others [10–14]. Wang and colleagues demonstrated that the biocompatibility and osteointegration of a polyethylene terephthalate (PET) artificial ligament were significantly improved by coating the material with HA via the plasma-spraying technique, increasing the proliferation of cells and upregulating the expression of bone formation-related genes [12]. Li and colleagues modified the PET ligament by the dip-coating method and found that a commercial HA coating on the PET ligament had a positive effect on the induction of artificial ligament osteointegration in the bone tunnel [15]. However, commercial HA cannot replace natural bone mineralization because of its inability to resemble HA crystals in natural bone [16].

Therefore, the objective of the present study was to biomineralize HA on a silk-collagen scaffold and assesses the effect of HA on osteointegration at the graft-bone

interface in an animal model of ACL reconstruction. Silk-collagen scaffolds with both ends modified by HA were used in a rabbit model of ACL reconstruction, and silk-collagen scaffolds were used as the control. The effects on osteointegration at the tendon-bone interface were verified by micro-CT, histology, and biomechanical testing. Meanwhile, the effects of the two scaffolds in terms of preventing osteoarthritis were also evaluated. The hypothesis is that the graft-bone healing process can be enhanced by HA biomineralization.

## Materials and methods

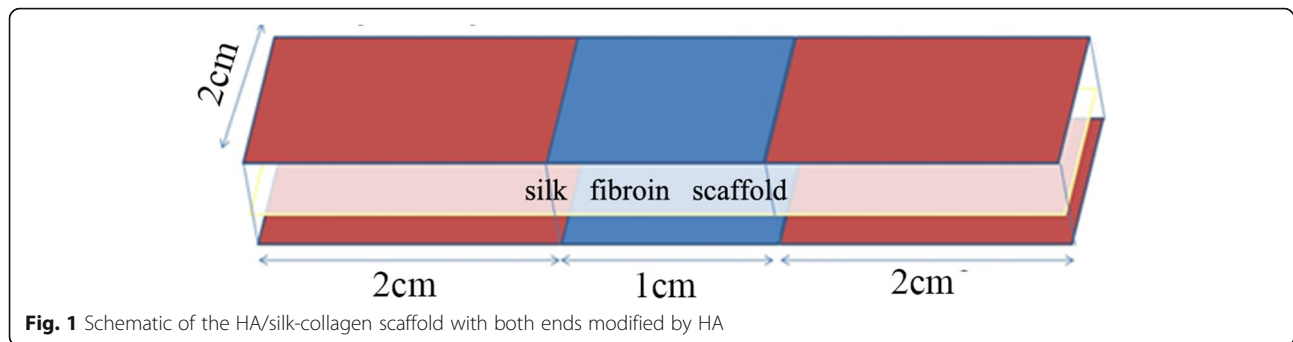
### Fabrication of silk-collagen scaffolds and HA/silk-collagen scaffolds

The fabrication of the silk-collagen scaffold has been previously described [2]. Briefly, raw silk fibers (*Bombyx mori*), provided by Zhejiang Cathaya International, Inc. (Hangzhou, China), were used to fabricate knitted scaffolds on a knitting machine. An aqueous solution containing 0.02 M Na<sub>2</sub>CO<sub>3</sub> was used to remove sericin, the glue-like protein adhering to silk fibroin, by incubation at 90°C and 100°C for 60 min. The type I collagen solution was extracted and refined by neutral salt and dilute acid extractions from pig Achilles' tendon. The silk fibroin scaffold was immersed in the collagen solution (15 mg/ml, 2 mm depth). It was frozen at -80°C and freeze-dried under vacuum for formation of the collagen sponge. Then, the scaffolds were crosslinked by dehydrothermal treatment [17]. Finally, the silk-collagen scaffolds were cut into rectangles 2×5 cm in size.

Once the rectangular silk-collagen scaffolds (2×5 cm) were obtained, the distal and proximal 2-cm ends were immersed in simulated body fluid (SBF) for 4 days to nucleate bone-like nanostructured nonstoichiometric HA into self-assembling on the collagen fibers, as occurs in the biological process of neo-ossification (Fig. 1). Finally, all scaffolds were sterilized with  $\gamma$  irradiation.

### Experimental design

Twenty-four male New Zealand white rabbits weighing 2.5–3.0 kg (12 weeks old) were used in the present study. The Animal Care and Use Committee of Zhengzhou University approved the study protocol. All methods were performed in accordance with the relevant guidelines and regulations. The animals were randomly divided into two groups to undergo ACL reconstruction in the left hindlimb: animals in the S group ( $n=12$ ) received silk-collagen scaffold, and those in the HA group ( $n=12$ ) received HA/silk-collagen scaffolds. At 16 weeks postoperatively, all rabbits were sacrificed; half of the specimens in each group ( $n=6$ ) were evaluated by micro-CT and biomechanical testing to determine osteointegration at the tendon-bone interface, and the other half ( $n=6$ ) were evaluated by hematoxylin and eosin staining,



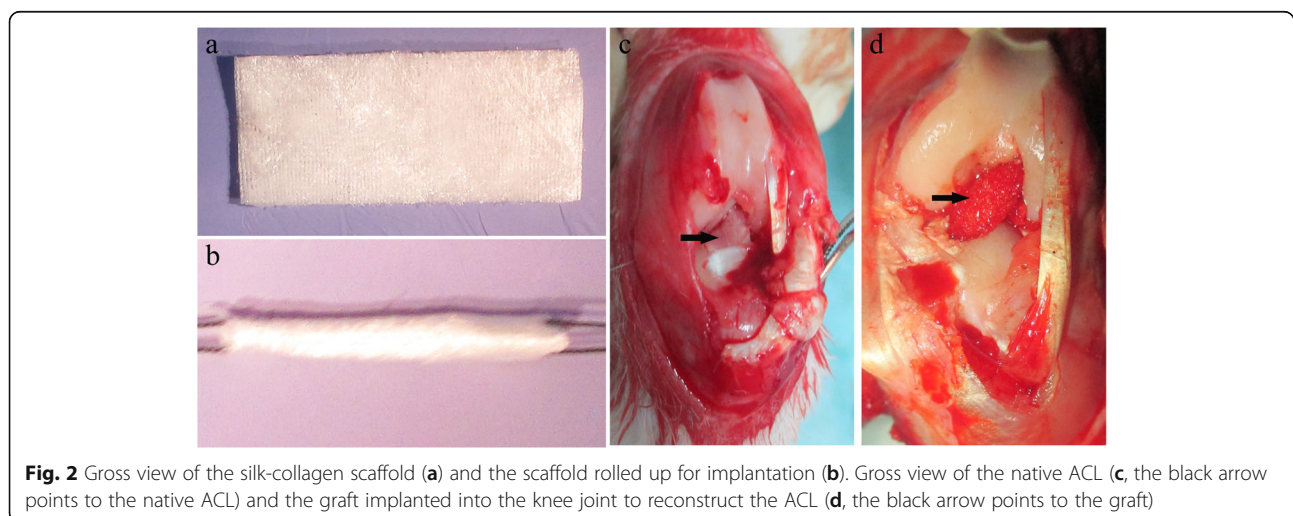
safranin O staining, and immunohistochemical staining for collagen I, collagen III, and osteocalcin. All the cartilage surfaces of the femoral condyles were harvested for the assessment of osteoarthritis prevention.

#### Surgical protocol

The surgical process of ACL reconstruction was performed under aseptic conditions. After general anesthesia was induced with an intravenous injection of pentobarbital sodium (30 mg/kg), the knee joint of the left hindlimb was exposed by lateral parapatellar arthrotomy. The native ACL was excised with a scalpel, and the tibial and femoral tunnels were created with a 2.0-mm drill at the ACL attachment site. The silk-collagen scaffold or HA/silk-collagen scaffold was carefully rolled up along the short axis to make a graft 2.0 mm in diameter and 50 mm in length. Then, the graft was passed through the bone tunnels, and both ends were fixed by sutures tied over screws in the tibia and femur. In the HA group, a 1-cm segment in the middle of the scaffold was ensured to be placed in the knee joint cavity. The incisions were sutured layer by layer, and all experimental animals were allowed to move freely in their cages postoperatively (Fig. 2a-d).

#### Histological and immunohistological assessment of the tendon-bone interface

To evaluate osteointegration at the tendon-bone interface, the tibia and femur ( $n=6$  for each group) were fixed in 10% paraformaldehyde immediately after collection. Then, the specimens were decalcified in 10% ethylenediaminetetraacetic acid (EDTA) for 4 weeks and embedded in paraffin. The sections along the longitudinal axis of the bone tunnel were cut at 5  $\mu\text{m}$  and stained with hematoxylin and eosin (HE) and safranin O for histological observation. For immunohistochemical staining, hydrogen peroxide was first used to block endogenous peroxidase. Then, the sections were treated with pepsin for 20 min. Monoclonal antibodies against collagen I (Abcam, England), collagen III (Chemicon), and osteocalcin (Abcam, England) were incubated with the sections at room temperature for 4 h. Then, the sections were incubated with biotinylated goat anti-mouse secondary antibody (Univ, Shanghai, China) at room temperature for 1 h. After streptavidin peroxidase was applied, 3,30-diaminobenzidine was utilized as a chromogenic agent, and hematoxylin was used for background staining. All staining and viewing procedures were performed under the same conditions, and typical sections were selected to assess osteointegration at the tendon-bone interface.



### Micro-CT

The specimens for micro-CT examination ( $n=6$  for each group) were stored at  $-80^{\circ}\text{C}$  immediately after harvest. Before the evaluation, the femur-graft-tibia complex was thawed to room temperature. Transverse, coronal, and sagittal images of the tibial bone tunnel were reconstructed by high-resolution micro-CT ( $36\ \mu\text{m}$  thickness with isotropic resolution, SkyScan 1176, Bruker, Belgium). Therefore, the osteointegration at the tendon-bone interface could be determined by screening all images of each specimen. A 3.0-mm-wide cylindrical volume of interest (VOI) was centered along the longitudinal axis of the tibial bone tunnel from the proximal to the distal attachment site (Fig. 3). The VOI contained the newly formed mineral tissue surrounding the tunnel and the graft because the tunnels were drilled with a 2.0-mm drill bit. All indexes, including the bone volume fraction (BV/TV, %), trabecular number (Tb.N, 1/mm), trabecular separation (Tb.Sp, mm), trabecular thickness (Tb.Th, mm), structure model index (SMI), and bone mineral density (BMD,  $\text{g}/\text{cm}^3$ ), were determined based on the total number of voxels and the number of bone voxels in the VOI.

### Biomechanical testing

Specimens were processed for biomechanical testing immediately after micro-CT ( $n=6$  for each group). Before testing, all soft tissue except the graft in the knee cavity and sutures at the tunnel exits was carefully removed to

eliminate confounding factors. The femur-graft-tibia complex was fixed in custom iron tubes that were clamped to a material testing machine (Instron 553A, USA, Fig. 4a). The preload was set at 1 N, and the tensile load continuously increased at a displacement rate of 20 mm/min. During the test, specimens were always kept moist with normal saline solution. The displacement and tensile load were recorded on the load-deformation curve, and stiffness could be calculated by the slope of the curve. We also recorded the site of graft failure (tibial tunnel, midsubstance, or femoral tunnel).

### Observation of osteoarthritis prevention

X-ray anteroposterior (A-P) photographs of the knee joint of the left hindlimb were captured using a Kodak-FX system at 40 kV for 5 ms. The distance between the tibial plateau and femoral condyles was measured to evaluate the level of osteoarthritis. The cartilage surface of the femoral condyles of the left hindlimb was stained with India ink for macroscopic observation [18]. Then, the specimens were fixed, decalcified, embedded in paraffin blocks, and sectioned at  $5\ \mu\text{m}$ . Subsequently, the sections were deparaffinized with xylene, hydrated with decreasing concentrations of alcohol, and then subjected to HE staining and safranin O staining. The modified Mankin score was used to evaluate osteoarthritis in the two groups [19].

### Statistical analyses

All quantitative data are expressed as the mean  $\pm$  standard deviation (SD), and differences in the results between the two groups were detected by Student's *t* test.  $P < 0.05$  was considered to indicate a significant difference.

## Results

### Gross observation

The native ACL in the knee cavity of the left hindlimb was removed at the attachment site and replaced by a rolled-up silk-collagen scaffold or HA/silk-collagen scaffold with both ends modified by HA. No signs of gross infection were observed in either group; all knee joints of the experimental limbs contained clear serous fluid. The regenerated ligament in the knee cavity resembled the native ACL in both groups at 16 weeks postoperatively. Abundant newly regenerated fibrous tissue filled the space in the scaffold, and silk fibers could be discerned. Additionally, a thin layer of synovium-like tissue was observed on the surface of the regenerated ligament in the knee cavity. The luster and color of the regenerated ligament glossy white throughout, which is similar to that of the native ACL.

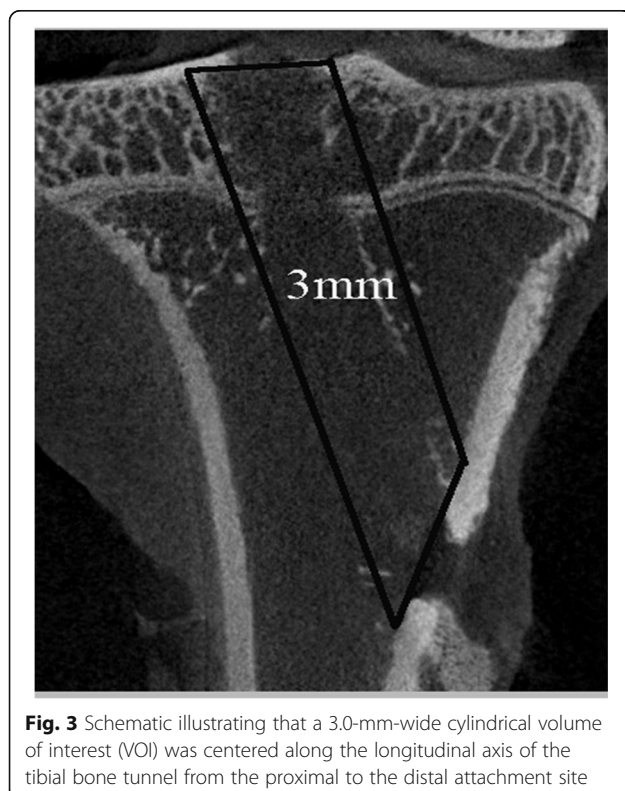


**Fig. 3** Schematic illustrating that a 3.0-mm-wide cylindrical volume of interest (VOI) was centered along the longitudinal axis of the tibial bone tunnel from the proximal to the distal attachment site



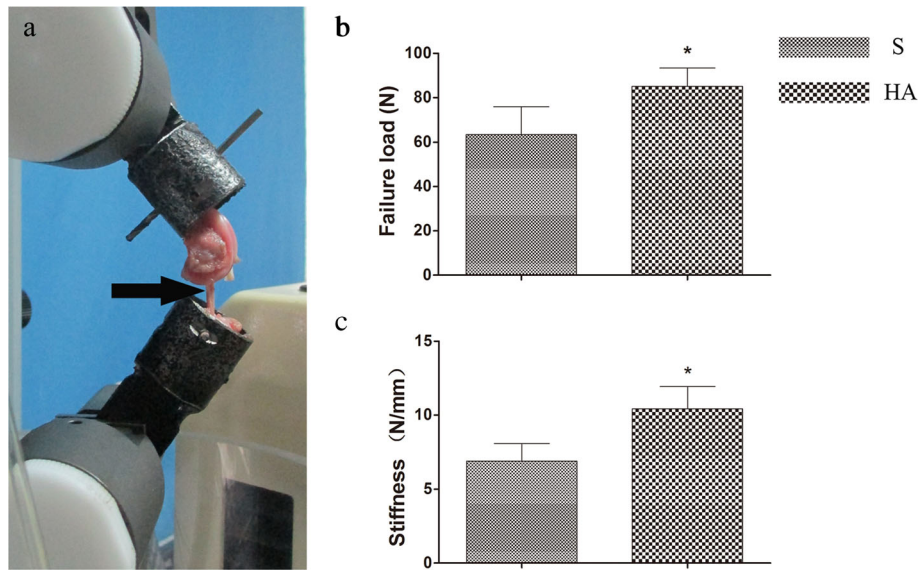


**Fig. 4** The femur-graft-tibia complex was fixed in custom iron tubes and clamped to an Instron machine for biomechanical testing (a, the black arrow points to the graft). The average failure load in the HA group was significantly greater than that in the S group at 16 weeks postoperatively (b). A significant difference in stiffness was also detected between the two groups (c). Asterisk indicates a significant difference between groups

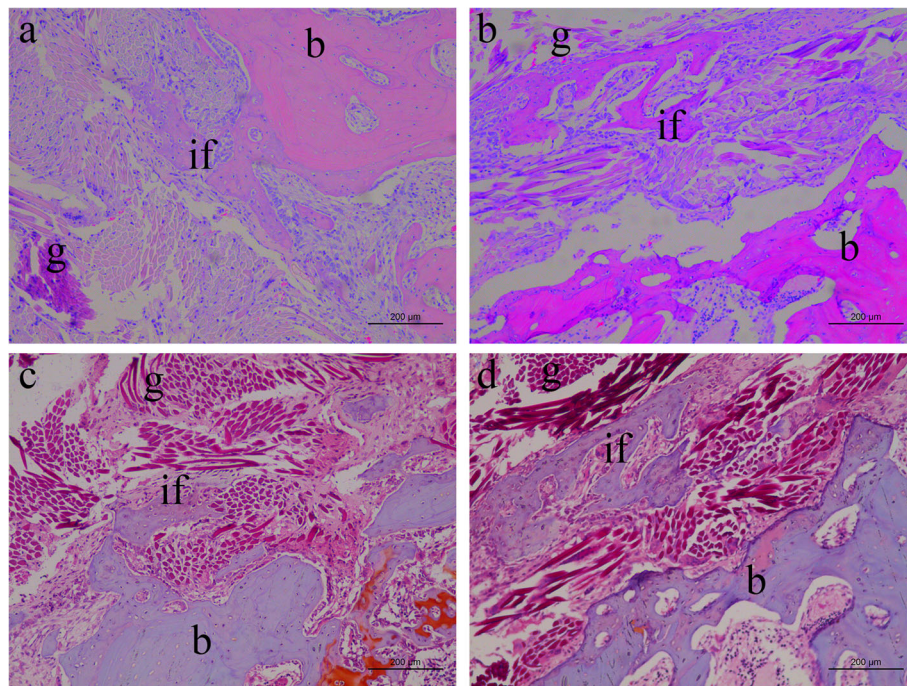


**Fig. 5** HE staining of the tendon-bone interface. Ingrowth of trabecular bone into the graft was observed in the S group, similar to the findings of our previous study (a). Massive trabecular bone formation in the core area of the graft was observed in the HA group (b). Safranin O staining revealed more mature osteointegration at the tendon-bone interface in the HA group (d) than in the S group (c). b, bone; if, interface; g, graft

### Histological and immunohistochemical staining

At 16 weeks postoperatively, much regenerated tissue could be seen in the core and peripheral areas of the grafts in both groups. The grafts showed close contact with the native tissue. In the S group, osteointegration was observed at the tendon-bone interface with bone ingrowth into the graft, as described in our previous study (Fig. 5a) [2]. In the HA group, more mature trabecular bone was observed in the deeper part of the graft, indicating that more osteointegration occurred (Fig. 5b). Moreover, safranin O staining provided clearer images of tissue regeneration and osteointegration. The grafts were surrounded by massive amounts of collagen and newly formed bone. More bone formation was clearly determined in the HA group than in the S group (Fig. 5c and d).

Immunohistochemical staining was used to evaluate extracellular matrix (ECM) production at the tendon-

bone interface. More collagen I deposition was observed in the HA group than in the S group, indicating progressive bone matrix regeneration (Fig. 6a and b). On the other hand, collagen III was expressed at a low level in the recovered area in the HA group (Fig. 6c and d). Osteocalcin is abundant in developing bone, and its faded staining in the HA group may implicate major recovery after implantation of the HA/silk-collagen scaffold (Fig. 6e and f).

### Micro-CT

Images of the bone tunnels were reconstructed by high-resolution micro-CT, and the newly regenerated mineralized tissue in the bone tunnels could be easily determined by screening all slices of each sample. At 16 weeks postoperatively, the micro-CT images showed a more obvious signal in the tibial bone tunnel in the HA

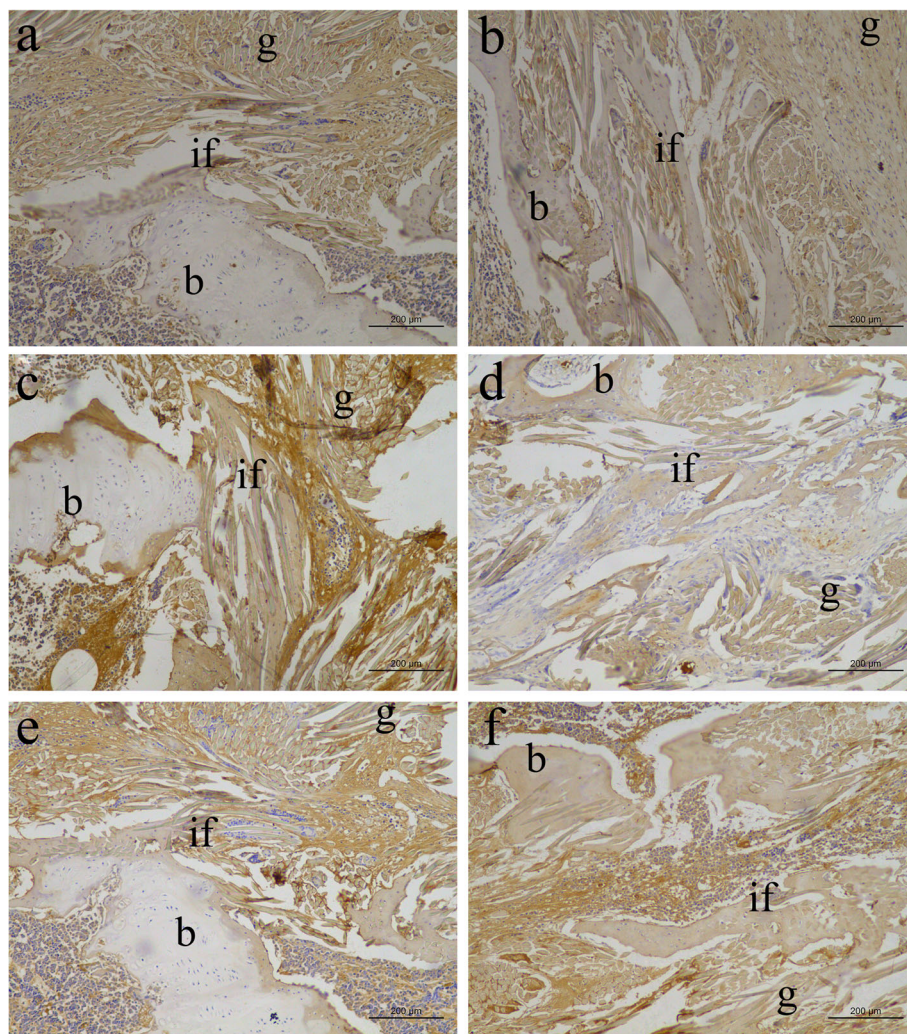


**Fig. 6** Immunohistochemical staining for collagen I (a, b), collagen III (c, d), and osteocalcin (e, f) in the S group (a, c, e) and HA group (b, d, f). b, bone; if, interface; g, graft

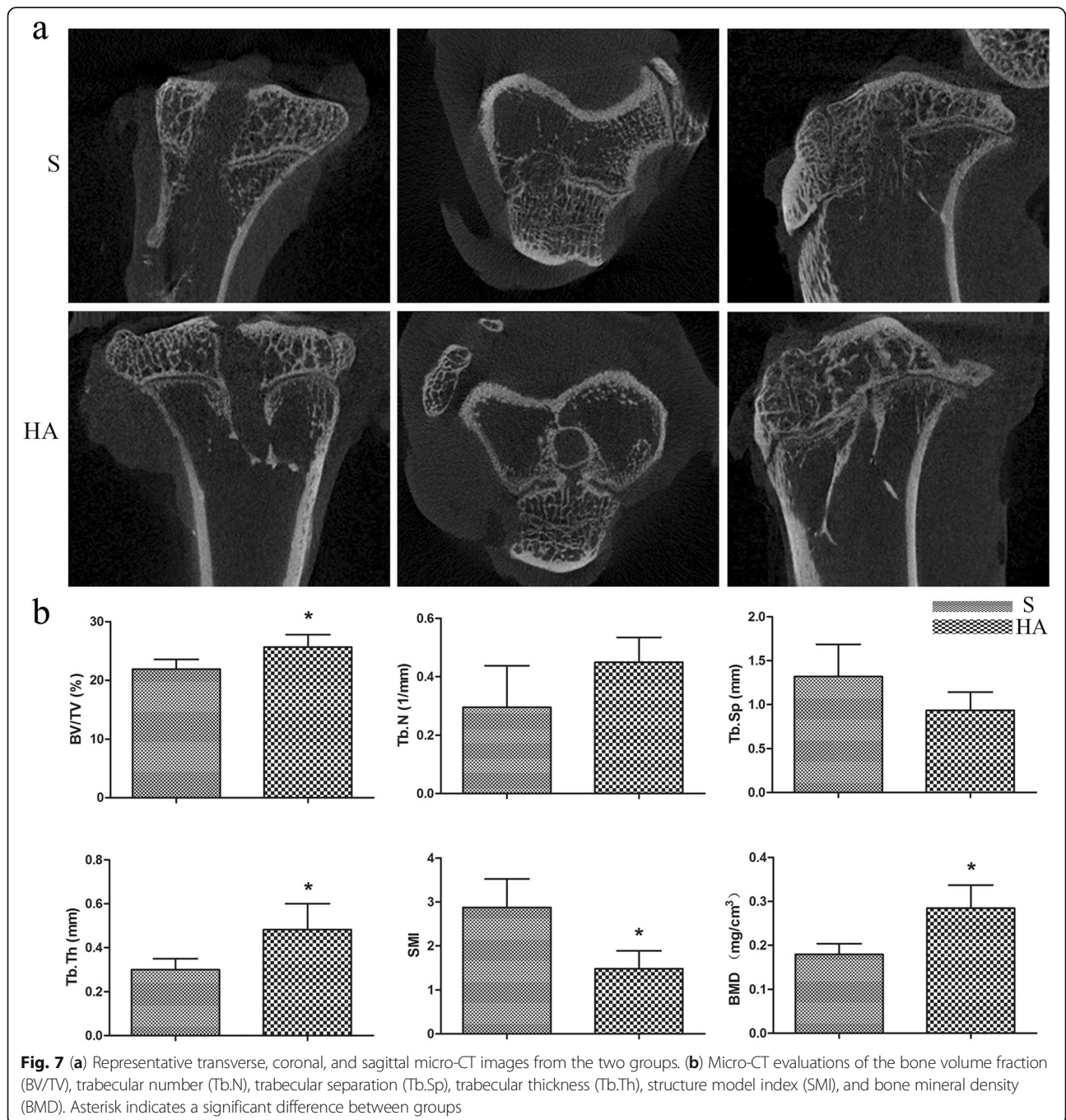


group than in the S group, indicating more mineralized tissue formation at the tendon-bone interface in the HA group (Fig. 7a). At 16 weeks postoperatively, the BV/TV of the VOI in the HA group was significantly greater than that in the S group ( $21.91 \pm 1.65$  for the S group and  $25.67 \pm 2.10$  for the HA group;  $p=0.006$ ). Meanwhile, there were also significant differences detected in the Tb.Th, SMI, and BMD in the HA group compared with the S group ( $p=0.006$ , 0.01, and 0.001, respectively). No significant difference in the Tb.N or Tb.Sp was detected

between the two groups ( $p=0.052$  and 0.056, respectively; Fig. 7b).

**Biomechanical testing**

In the evaluation of the failure mode, all grafts in both groups failed by partially tearing inside the bone tunnel at 16 weeks postoperatively. The average load to failure in the HA group was significantly greater than that in the S group (HA,  $85.07 \pm 8.30$  vs. S,  $63.47 \pm 12.65$  N;  $p < 0.05$ ; Fig. 4b). A significant difference in stiffness was



also detected between the two groups (HA,  $10.42 \pm 1.51$  vs. S,  $6.89 \pm 1.19$  N/mm;  $p < 0.05$ ; Fig. 4c).

### Prevention of osteoarthritis

Cartilage always degenerates following injuries to the ACL, and an effective therapeutic method should prevent osteoarthritis in addition to regenerating the ACL. Radiological analyses were performed to compare joint knee degeneration between the two groups. Radiographic images demonstrated that joints in the HA group maintained a normal joint space with fewer osteophytes than joints in the S group, indicating that implantation of the HA/silk-collagen scaffold resulted in a more stable joint than that of the silk-collagen scaffold (Fig. 8a). At 16 weeks postoperatively, distinct abrasion of the femoral condyles was observed in the S group, as evidenced by intense staining with India ink (Fig. 8b). The articular surface was less affected in the HA group. Histological images (HE and safranin O staining) showed a regular and smooth articular surface with minimal roughness in the HA group. However, clear fissures and visible fibrillation were present in the S group, which was consistent with the macroscopic results, and weakly stained cartilage of the articular surface was also observed (Fig. 8c and d). The average Mankin score in the HA group was significantly lower than that in the S group, revealing slower degeneration of articular cartilage in the HA group (Fig. 8e).

### Discussion

Applications of cytokines/growth factors and bone marrow mesenchymal stem cells (BMSCs) have become very popular in tissue engineering, especially for spinal fusion and tendon/ligament regeneration [20–23]. However, many problems exist when these technologies are applied in vivo; for example, the final fate of the implanted cells is not clear. However, it has been reported that BMSCs remodel themselves to secrete more extracellular matrix (ECM), which is suitable for ligament regeneration, when they are implanted on silk fibroin scaffolds [24]. Additionally, more ECM deposition for bone formation at the tendon-bone interface is expected after ACL reconstruction [25]. Therefore, the applications of BMSCs and scaffolds need to be modified for better results. Recently, the codelivery and controlled release of cytokines/growth factors with scaffolds has become a trend in tissue engineering, and BMP-2 is an often-used factor for bone regeneration [26–29]. A BMP-2-loaded, bioactive and bioresorbable scaffold fabricated from caprolactone and  $\beta$ -tricalcium phosphate could act as a graft substitute by providing a suitable environment for bone regeneration in a porcine model of interbody spinal fusion [20]. Although bone formation was promoted, several concerns remain, such as the easy loss of

cytokine/growth factor bioactivity because of rapid diffusion and microenvironmental changes, dosages being much higher than normal, and the cascade effects continuing to be controversial [30, 31]. Some cytokines/growth factors can cause massive inflammatory reactions when implanted systemically into patients with contraindications [30].

Key components of successful osteointegration at the tendon-bone interface include a biocompatible scaffold fit to the bone interface, progenitor cells, and osteoinductive factors. In our previous study, the silk-collagen scaffold was proven to be a biocompatible scaffold that induced cell infiltration for ligament regeneration and bone ingrowth for tendon-bone healing [2]. Second, host cells around defects that contain BMSCs mainly contribute to initiating and regulating the tendon-bone healing process [32, 33]. HA has been demonstrated to be an effective osteoinductive factor by in vitro and in vivo trials. Therefore, the biomaterial can promote osteointegration at the tendon-bone interface on the material aspect, avoiding the defects of implanted cytokines/growth factors and BMSCs.

Successful ACL reconstruction requires solid tendon-bone healing, but the healing process is slow because the graft in the bone tunnel is separated from the vascular supply and because there is bone loss at the site of injury. During healing, the structure and composition of the native direct tendon-bone interface is not formed, a structurally and biomechanically inferior interface is formed [34]. Previous studies have demonstrated that osteoinductive agents accelerate osteointegration of the tendon graft, with improved tendon-bone healing and mechanical properties [35–37], as does HA [38, 39]. HE and safranin O staining showed that the wounds in the bone tunnel had already recovered in the two groups at 16 weeks postoperatively. The implanted graft and native tissue were tightly connected with each other. New bone tissue grew into the core part of the graft, and a massive amount of trabecular bone was discovered. The results in the S group were similar to our previous findings at 16 weeks postoperatively, and those in the HA group indicated faster bone integration. High cell viability was observed in the two groups, while the scaffold used in the present study did not contain any cells, which further illustrated that implanted cells are not essential for bone integration. Immunohistological staining for collagen I, collagen III, and osteocalcin was performed to further characterize bone integration. Strong collagen I deposition at the tendon-bone interface was observed. The newly formed tissues surrounding the scaffold indicated that the HA/silk-collagen scaffold can promote maturation of the bone matrix. Collagen III is one component of ligament and tendon tissues. Its amount will increase when injured tissues regenerate and remodel



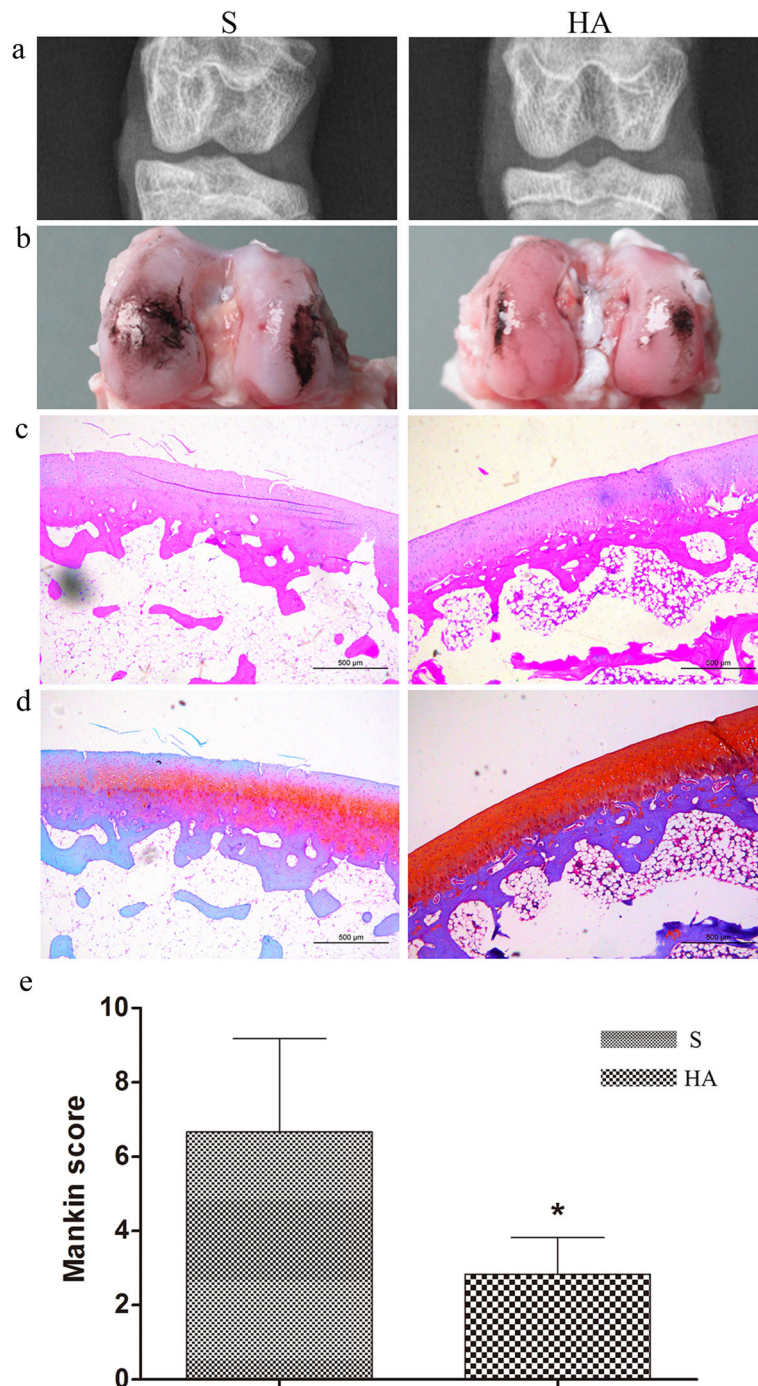


**Fig. 8** (a) Radiological analysis of the knee joint after treatment with the silk-collagen scaffold (S) and HA/silk-collagen scaffold (HA). (b) Gross observation of the cartilage surface of the femoral condyles stained with India ink to show the defects. (c) HE staining and (d) Safranin O staining of the cartilage surface of the femoral condyles. (e) Histological evaluation according to the Mankin scoring system. Asterisk indicates a significant difference between groups

and will decrease when the tissues fully regenerate [40, 41]. Therefore, stronger staining was observed in the S group than in the HA group, indicating a slower transition from ligament to bone tissue. Osteocalcin is a marker of terminal osteoblast differentiation influencing

bone mineralization [42]. The higher osteocalcin density in the HA group indicated the efficacy of HA/silk in osteogenesis.

The amount of newly formed bone in the tibial tunnels was determined by micro-CT. Micro-CT has been used

to evaluate mineralized tissue formation in a rotator cuff model [43], and we used it to determine the amount of bone formed in a tunnel, as in a previous study [9]. Higher BV/TV, Tb.Th and BMD values, which reflect the volume of newly formed bone and thickness of trabecular bone, were detected in the HA group than in the S group. The walls of the bone tunnel in the HA group showed more newly formed bone than those in the S group. The newly formed bone can facilitate direct bonding between the bone and the graft and prevent knee instability associated with bone tunnel enlargement. Bone tunnel enlargement in the knee joint due to bone resorption is a common problem after ACL reconstruction [44]. The new bone formation in the HA group could be more effective in terms of long-term function by preventing joint instability associated with bone tunnel enlargement, according to the present results.

The failure load in the HA group was larger than that in the S group at 16 weeks postoperatively, and a significantly higher stiffness was detected in the HA group. The results of the biomechanical tests were consistent with the histological and radiological findings. When autografts are used to reconstruct the ACL, the tendon-bone healing process comprises a series of cellular events with an orderly transition of graft cell necrosis and host cell ingrowth [33]. The cell types that initiate and regulate tendon-bone healing have not yet been concretely identified [45], and it seems that host cells from the surrounding bone marrow, which contains pre-osteoblasts, contribute to osteointegration at the tendon-bone interface [32, 33]. In the present study, significant differences in the failure load and stiffness between the HA group and the S group were observed, indicating that the HA on the scaffold exerted an osteoconductive effect on the tendon-bone healing process.

In the present study, osteoarthritis progression following ACL reconstruction was investigated. Osteophyte formation, the joint space width, and the articular surface, which are always disrupted by instability of the knee joint, were assessed by radiological and histological methods. Osteoarthritis was more severe in the S group than in the HA group. Inhibition of the progression of osteoarthritis in the HA group is likely because the HA/silk-collagen scaffold promoted tendon-bone healing, which enhanced joint stability and reduced meniscal injury. Therefore, the results of osteoarthritis occurrence provide comprehensive evidence illustrating that the HA/silk-collagen scaffold can induce better osteointegration at the tendon-bone interface and greater joint stability.

There are some limitations to our study. The animal model we used may not fully mimic human physiological conditions. Additionally, only one time point was selected to evaluate tendon-bone healing, preventing the evaluation of recovery and remodeling throughout the osteointegration process.

## Conclusion

In our present study, an HA/silk-collagen scaffold was fabricated and demonstrated to promote osteointegration at the tendon-bone interface after ACL reconstruction. The HA/silk-collagen scaffold is a promising promoter of osteointegration, as observed in animal trials. Future larger animal and clinical trials are needed.

## Supplementary Information

The online version contains supplementary material available at <https://doi.org/10.1186/s13018-021-02281-0>.

**Additional file 1: Supplementary data.** Comparison of the micro-CT results and biomechanical test results from the two groups.

## Abbreviations

ACL: Anterior cruciate ligament; HA: Hydroxyapatite; SBF: Simulated body fluid; ECM: Extracellular matrix; EDTA: Ethylenediaminetetraacetic acid; HE: Hematoxylin and eosin; VOI: Volume of interest; BV/TV: Bone volume fraction; Tb.N: Trabecular number; Tb.Sp: Trabecular separation; Tb.Th: Trabecular thickness; SMI: Structure model index; BMD: Bone mineral density; SD: Standard deviation; BMSCs: Bone marrow mesenchymal stem cells; BMP: Bone morphogenetic protein

## Acknowledgements

This work was supported by the Foundation of Henan Educational Committee (19A320011), the Key Project of Science and Technology Department of Henan Province-2020 (22170139), and the Youth Fund of the First Affiliated Hospital of Zhengzhou University.

## Authors' contributions

Conceived and designed the experiment: Fanggang Bi and Ke Tian; performed the experiments: Fanggang Bi, Yangdi Chen, Yafei Wang, Junqi Liu, and Danfeng Xu; analyzed the data: Fanggang Bi and Yangdi Chen; contributed reagents/materials/analysis tools: Fanggang Bi and Ke Tian; wrote the manuscript: Fanggang Bi. The author(s) read and approved the final manuscript.

## Funding

This work was supported by the Foundation of Henan Educational Committee (19A320011), the Key Project of Science and Technology Department of Henan Province-2020 (22170139), and the Youth Fund of the First Affiliated Hospital of Zhengzhou University.

## Availability of data and materials

All the data of the manuscript are presented in the paper or additional supporting files.

## Ethics approval and consent to participate

The Animal Care and Use Committee of Zhengzhou University approved the study protocol. All methods were performed in accordance with the relevant guidelines and regulations.

## Consent for publication

Not applicable.

## Competing interests

The authors declare that they have no competing interests.

## Author details

<sup>1</sup>Department of Orthopedic Surgery, The First Affiliated Hospital of Zhengzhou University, NO.1 Jianshe East Road, Zhengzhou 450001, China. <sup>2</sup>Henan University of Chinese Medicine, NO.156 Jinshui East Road, Zhengzhou 450001, China. <sup>3</sup>Department of Radiation Oncology, The First Affiliated Hospital of Zhengzhou University, NO.1 Jianshe East Road, Zhengzhou 450001, China. <sup>4</sup>Department of Orthopedic Surgery, Shaoying Central Hospital, NO.1 Huayu Road, Shaoying 312000, China.

Received: 24 November 2020 Accepted: 4 February 2021  
Published online: 16 February 2021

## References

- Kim HS, Seon JK, Jo AR. Current trends in anterior cruciate ligament reconstruction. *Knee Surg Related Res.* 2013;25(4):165–73.
- Bi F, Shi Z, Liu A, Guo P, Yan S. Anterior cruciate ligament reconstruction in a rabbit model using silk-collagen scaffold and comparison with autograft. *PLoS One.* 2015;10(5):e0125900.
- Maak TG, Voos JE, Wickiewicz TL, Warren RF. Tunnel widening in revision anterior cruciate ligament reconstruction. *J Am Acad Orthop Surg.* 2010;18(11):695–706.
- Kaeding CC, Aros B, Pedroza A, Pifel E, Amendola A, Andrich JT, Dunn WR, Marx RG, McCarty EC, Parker RD, et al. Allograft versus autograft anterior cruciate ligament reconstruction: predictors of failure from a MOON prospective longitudinal cohort. *Sports Health.* 2011;3(1):73–81.
- Petrigliano FA, McAllister DR, Wu BM. Tissue engineering for anterior cruciate ligament reconstruction: a review of current strategies. *Arthroscopy.* 2006;22(4):441–51.
- Ge Z, Yang F, Goh JC, Ramakrishna S, Lee EH. Biomaterials and scaffolds for ligament tissue engineering. *J Biomed Mater Res A.* 2006;77(3):639–52.
- Altman GH, Diaz F, Jakuba C, Calabro T, Horan RL, Chen J, Lu H, Richmond J, Kaplan DL. Silk-based biomaterials. *Biomaterials.* 2003;24(3):401–16.
- Liu H, Fan H, Wang Y, Toh SL, Goh JC. The interaction between a combined knitted silk scaffold and microporous silk sponge with human mesenchymal stem cells for ligament tissue engineering. *Biomaterials.* 2008;29(6):662–74.
- Tien YC, Chih TT, Lin JH, Ju CP, Lin SD. Augmentation of tendon-bone healing by the use of calcium-phosphate cement. *J Bone Joint Surg (Br).* 2004;86(7):1072–6.
- Kaushik N, Nhat Nguyen L, Kim JH, Choi EH, Kumar Kaushik N. Strategies for using polydopamine to induce biomineralization of hydroxyapatite on implant materials for bone tissue engineering. *Int J Mol Sci.* 2020;21(18).
- Capuccini C, Torricelli P, Sima F, Boanini E, Ristoscu C, Bracci B, Socol G, Fini M, Mihailescu IN, Bigi A. Strontium-substituted hydroxyapatite coatings synthesized by pulsed-laser deposition: in vitro osteoblast and osteoclast response. *Acta Biomater.* 2008;4(6):1885–93.
- Wang S, Ge Y, Ai C, Jiang J, Cai J, Sheng D, Wan F, Liu X, Hao Y, Chen J, et al. Enhance the biocompatibility and osseointegration of polyethylene terephthalate ligament by plasma spraying with hydroxyapatite in vitro and in vivo. *Int J Nanomedicine.* 2018;13:3609–23.
- Liu F, Wang X, Chen T, Zhang N, Wei Q, Tian J, Wang Y, Ma C, Lu Y. Hydroxyapatite/silver electrospun fibers for anti-infection and osteoinduction. *J Adv Res.* 2020;21:91–102.
- Asri RI, Harun WS, Hassan MA, Ghani SA, Buyong Z. A review of hydroxyapatite-based coating techniques: Sol-gel and electrochemical depositions on biocompatible metals. *J Mech Behav Biomed Mater.* 2016;57:95–108.
- Li H, Ge Y, Wu Y, Jiang J, Gao K, Zhang P, Wu L, Chen S. Hydroxyapatite coating enhances polyethylene terephthalate artificial ligament graft osseointegration in the bone tunnel. *Int Orthop.* 2011;35(10):1561–7.
- Cai J, Ai C, Chen J, Chen S. Biomineralization of hydroxyapatite on polyethylene terephthalate artificial ligaments promotes graft-bone healing after anterior cruciate ligament reconstruction: an in vitro and in vivo study. *J Biomater Appl.* 2020;35(2):193–204.
- Torres DS, Freyman TM, Yannas IV, Spector M. Tendon cell contraction of collagen-GAG matrices in vitro: effect of cross-linking. *Biomaterials.* 2000;21(15):1607–19.
- Yoshioka M, Shimizu C, Harwood FL, Coutts RD, Amiel D. The effects of hyaluronan during the development of osteoarthritis. *Osteoarthr Cartil.* 1997;5(4):251–60.
- Armstrong S, Read R, Ghosh P. The effects of intraarticular hyaluronan on cartilage and subchondral bone changes in an ovine model of early osteoarthritis. *J Rheumatol.* 1994;21(4):680–8.
- Abbah SA, Lam CX, Huttmacher DW, Goh JC, Wong HK. Biological performance of a polycaprolactone-based scaffold used as fusion cage device in a large animal model of spinal reconstructive surgery. *Biomaterials.* 2009;30(28):5086–93.
- Heng NH, Zahlten J, Cordes V, Ong MM, Goh BT, N'Guessan PD, Pischon N. Effects of enamel matrix derivative and transforming growth factor-beta1 on connective tissue growth factor in human periodontal ligament fibroblasts. *J Periodontol.* 2015;86(4):569–77.
- de Albornoz PM, Aicale R, Forriol F, Maffulli N. Cell therapies in tendon, ligament, and musculoskeletal system repair. *Sports Med Arthrosc Rev.* 2018;26(2):48–58.
- Rizzello G, Longo UG, Petrillo S, Lamberti A, Khan WS, Maffulli N, Denaro V. Growth factors and stem cells for the management of anterior cruciate ligament tears. *Open Orthop J.* 2012;6:525–30.
- Chen JL, Yin Z, Shen WL, Chen X, Heng BC, Zou XH, Ouyang HW. Efficacy of hESC-MSCs in knitted silk-collagen scaffold for tendon tissue engineering and their roles. *Biomaterials.* 2010;31(36):9438–51.
- Fan H, Liu H, Wong EJ, Toh SL, Goh JC. In vivo study of anterior cruciate ligament regeneration using mesenchymal stem cells and silk scaffold. *Biomaterials.* 2008;29(23):3324–37.
- Perez RA, Kim JH, Buitrago JO, Wall IB, Kim HW. Novel therapeutic core-shell hydrogel scaffolds with sequential delivery of cobalt and bone morphogenetic protein-2 for synergistic bone regeneration. *Acta Biomater.* 2015;23:295–308.
- Kim IG, Hwang MP, Du P, Ko J, Ha CW, Do SH, Park K. Bioactive cell-derived matrices combined with polymer mesh scaffold for osteogenesis and bone healing. *Biomaterials.* 2015;50:75–86.
- Subramanian G, Bialorucki C, Yildirim-Ayan E. Nanofibrous yet injectable polycaprolactone-collagen bone tissue scaffold with osteoprogenitor cells and controlled release of bone morphogenetic protein-2. *Mater Sci Eng C Mater Biol Appl.* 2015;51:16–27.
- Ribeiro FO, Gomez-Benito MJ, Folgado J, Fernandes PR, Garcia-Aznar JM. In silico Mechano-chemical model of bone healing for the regeneration of critical defects: the effect of BMP-2. *PLoS One.* 2015;10(6):e0127722.
- Ritting AW, Weber EW, Lee MC. Exaggerated inflammatory response and bony resorption from BMP-2 use in a pediatric forearm nonunion. *J Hand Surg.* 2012;37(2):316–21.
- Shi P, Chen K, Goh JC. Efficacy of BMP-2 delivery from natural protein based polymeric particles. *Adv Healthc Mater.* 2013;2(7):934–9.
- Kawamura S, Ying L, Kim HJ, Dynybil C, Rodeo SA. Macrophages accumulate in the early phase of tendon-bone healing. *J Orthop Res.* 2005;23(6):1425–32.
- Kobayashi M, Watanabe N, Oshima Y, Kajikawa Y, Kawata M, Kubo T. The fate of host and graft cells in early healing of bone tunnel after tendon graft. *Am J Sports Med.* 2005;33(12):1892–7.
- Rothrauff BB, Tuan RS. Cellular therapy in bone-tendon interface regeneration. *Organogenesis.* 2014;10(1):13–28.
- Rodeo SA, Suzuki K, Deng XH, Wozney J, Warren RF. Use of recombinant human bone morphogenetic protein-2 to enhance tendon healing in a bone tunnel. *Am J Sports Med.* 1999;27(4):476–88.
- Martinek V, Latterman C, Usas A, Abramowitch S, Woo SL, Fu FH, Huard J. Enhancement of tendon-bone integration of anterior cruciate ligament grafts with bone morphogenetic protein-2 gene transfer: a histological and biomechanical study. *J Bone Joint Surg Am.* 2002;84-a(7):1123–31.
- Chen CH, Liu HW, Tsai CL, Yu CM, Lin IH, Hsueh GH. Photoencapsulation of bone morphogenetic protein-2 and periosteal progenitor cells improve tendon graft healing in a bone tunnel. *Am J Sports Med.* 2008;36(3):461–73.
- Chung EJ, Sugimoto MJ, Koh JL, Ameer GA. A biodegradable tri-component graft for anterior cruciate ligament reconstruction. *J Tissue Eng Regen Med.* 2017;11(3):704–12. <https://doi.org/10.1002/term.1966>.
- Jiang J, Wan F, Yang J, Hao W, Wang Y, Yao J, Shao Z, Zhang P, Chen J, Zhou L, et al. Enhancement of osseointegration of polyethylene terephthalate artificial ligament by coating of silk fibroin and depositing of hydroxyapatite. *Int J Nanomedicine.* 2014;9:4569–80.
- Kumada Y, Zhang S. Significant type I and type III collagen production from human periodontal ligament fibroblasts in 3D peptide scaffolds without extra growth factors. *PLoS One.* 2010;5(4):e10305.
- Chamberlain CS, Crowley EM, Kobayashi H, Eliceiri KW, Vanderby R. Quantification of collagen organization and extracellular matrix factors within the healing ligament. *Microsc Microanal.* 2011;17(5):779–87.
- Oka S, Matsumoto T, Kubo S, Matsushita T, Sasaki H, Nishizawa Y, Matsuzaki T, Saito T, Nishida K, Tabata Y, et al. Local administration of low-dose simvastatin-conjugated gelatin hydrogel for tendon-bone healing in anterior cruciate ligament reconstruction. *Tissue Eng Part A.* 2013;19(9-10):1233–43.



43. Meyer DC, Jacob HA, Pistoia W, von Roll A, Gerber C. The use of acrylic bone cement for suture anchoring. *Clin Orthop Relat Res.* 2003;410:295–302.
44. Rodeo SA, Kawamura S, Ma CB, Deng XH, Sussman PS, Hays P, Ying L. The effect of osteoclastic activity on tendon-to-bone healing: an experimental study in rabbits. *J Bone Joint Surg Am.* 2007;89(10):2250–9.
45. Bi F, Shi Z, Jiang S, Guo P, Yan S. Intermittently administered parathyroid hormone [1-34] promotes tendon-bone healing in a rat model. *Int J Mol Sci.* 2014;15(10):17366–79.

### **Publisher's Note**

Springer Nature remains neutral with regard to jurisdictional claims in published maps and institutional affiliations.

**Ready to submit your research? Choose BMC and benefit from:**

- fast, convenient online submission
- thorough peer review by experienced researchers in your field
- rapid publication on acceptance
- support for research data, including large and complex data types
- gold Open Access which fosters wider collaboration and increased citations
- maximum visibility for your research: over 100M website views per year

**At BMC, research is always in progress.**

Learn more [biomedcentral.com/submissions](https://biomedcentral.com/submissions)

